THE AMERICAN SOCIETY OF MECHANICAL ENGINEERS
Three Park Avenue, New York, N.Y. 10016-5990

99-GT-275

The Calculation of Thermodynamic Non Equilibrium Combustion Product Compositions

C. D. Hurley*, M. Whiteman and C. W. Wilson
Combustion and Emissions Section, Propulsion Department, DERA, DERA Pyestock, Farnborough, United Kingdom, GU14 0LS.

Abstract

A method is presented by which the product composition and temperature of constant pressure combustion reactions can be calculated for non equilibrium conditions, by constraining the products free energy and entropy. The calculations for a hydrogen/ oxygen system are compared with chemical kinetic predictions. From the calculated compositions the relationship between free energy and extent of reaction are derived and thence how the individual product mole fractions vary with extent of reaction. The application of these techniques to modelling combustion chemistry is discussed.

Introduction

The principal chemical model used in computational fluid dynamic (CFD) modelling of combusting flows is based on chemical equilibrium. For a given fuel and oxidant, if their concentrations are known together with the system temperature and pressure, the chemical composition and final temperature of the combustion reaction can be calculated. Combustion product concentrations and product mixture temperatures are held as functions of the oxidant to fuel ratio (o/f). This is usually expressed as a mixture fraction (mf) where:

$$mf = \frac{1}{o/f + 1} \qquad (1)$$

mf is used for computational convenience since it varies between 0 and 1 and does not give rise to infinity when only oxidant is present. The CFD solution, for a given point, would contain fluid flow data including the mf probability density function (pdf); this describes how the mixture fraction at that point varies due to the turbulence of the system. By combining this pdf with the product and temperature functions of mf, the individual pdf's can be calculated which, when integrated, give the final product concentrations and temperature at that point.

The most widely used calculation procedure is that of Gordon and McBride (1994). This model makes few assumptions, is robust and can handle a wide range of fuels and oxidants over a wide temperature range (200 to 6000K). Its flexibility is only limited by the number of chemical species, and their associated chemical and thermodynamic data, stored in the programs data libraries. Many years of development have refined the model so that it can handle complex fuels, oxidants and product distributions including condensed phases.

The principal limitation of equilibrium models is the assumption of chemical equilibrium itself. In real combusting systems equilibrium is not achieved. Measurements of chemical compositions inside gas turbine combustors made at DERA have shown that in fuel rich regions of the flame the chemical compositions are considerably different to equilibrium. Figure 1 (Hurley 1994) summarises this by showing the differences between the measured and equilibrium concentrations of CO_2, CO and H_2 for a kerosene air flame at 7 bar and an inlet air temperature of 800K. Measurements approach equilibrium for lean mixtures (mf < 0.04). In richer mixtures (mf > 0.1) CO and H_2 are over-predicted and CO_2 under-predicted. Similarly both hydrocarbon and solid carbon (soot) concentrations are much greater than equilibrium predictions (Hurley 1994). For mf < 0.02, in the combustor exhaust, temperatures, calculated from the measured gas composition, agree well with equilibrium predictions. However despite this agreement, on closer examination of the measured product compositions, deviations from equilibrium can still be seen. Measured compositions have higher concentrations of CO and unburned hydrocarbons (HC) and much lower concentrations of oxides of nitrogen (NOx) than predicted by equilibrium calculations (Hurley 1994). Inaccurate estimates of temperature and composition will lead to errors in the computation of the flow field, principally due to inaccurate estimation of local gas densities. Therefore there is a case for developing a non equilibrium chemical model which could compensate for these errors. Such a model would combine the simplicity and flexibility of the equilibrium model but more accurately predict compositions temperature and densities in rich regions of the flame and pollutant emissions in combustor exhausts. Rather than write a computer program from scratch it was decided to modify the latest NASA Lewis equilibrium code, Chemical Equilibrium Applications (CEA) (Gordon and McBride 1994).

Presented at the International Gas Turbine & Aeroengine Congress & Exhibition
Indianapolis, Indiana — June 7–June 10, 1999

This paper details changes made to subroutines of CEA in order to obtain solutions other than equilibrium. To simplify the interpretation of the programs diagnostic output and to aid comparisons with chemical kinetic calculations, the non equilibrium program was developed on a simple hydrogen/oxygen system. However modifications were made in such a way as not to interfere with the generality of the program.

CURRENT EQUILIBRIUM CODE

General

The principal of operation of CEA is that for a given set of reactants (fuel and oxidant) and chemical reaction conditions (temperature, pressure etc.) the equilibrium product composition will be that combination of products that has the lowest energy. Here by energy is meant the thermodynamic energy which, at constant temperature and pressure, as in the case of gas turbine combustion, is the Gibbs free energy (G). Since G is a function of temperature solving for a minimum in G also determines the final temperature of the system. The following sections outline how CEA works in more detail. The product species can exist in all three phases solid, liquid or gas. In order to simplify modifications to the calculation, in this initial phase only gaseous products will be considered.

Minimisation technique

For a mixture of NG gases the free energy per kilogram of mixture is given by:

$$G = \sum_{j=1}^{NG} \mu_j n_j \qquad (2)$$

Where μ_j is the chemical potential or partial molar free energy per kilogram-mole of species j and n_j the number of kilogram-moles of species j per kilogram of mixture. The condition for equilibrium is the minimisation of this function. However, there is another condition that must simultaneously be met, that the reactants and products must be in mass balance i.e. the quantitative elemental composition of the products must be the same as that of the reactants.

$$\sum_{j=1}^{NG} a_{ij} nj - b_j^0 = 0 \qquad (3)$$

Where a_{ij} is the number of kilogram-atoms of element i per kilogram-mole of species j and b_j^0 is the number of kilogram-atoms of i per kilogram of total reactants. For a stationary point (min or max) if two conditions are to be satisfied simultaneously they can be linked by Lagrangian multipliers (λ_i). If this is done and the resulting equation differentiated with respect to n_j then the condition for a minimum becomes:

$$\sum_{j=1}^{NG} \left(\mu_j + \sum_{i=1}^{l} \lambda_i a_{ij} \right) = 0 \qquad (4)$$

Where l is the number of chemical elements in the system. Two further equations defining the system can be added to 3 and 4. If n is defined as the total number of kilogram-moles per kilogram of product mixture then this must equal the sum of the product n_j's

$$\sum_{j=1}^{NG} n_j - n = 0 \qquad (5)$$

and

$$H = H_0 \qquad (6)$$

where H and H_0 are the specific enthalpies (internal energy at constant pressure) of the products and reactants respectively. Equation 6 is merely a statement that the reaction is adiabatic. The four equations 3 to 6 are used in conjunction with a Newton Raphson method of iteratively finding a minimum by successive approximations. The technique involves Taylor series expansions of the equations with all terms truncated that contain derivatives higher than the first. Logarithmic forms of the correction variables are used for arithmetic convenience and all relevant terms are non-dimensionalised (to make the calculation independent of units) by dividing by RT, where R is the gas constant and T the absolute temperature of the product mixture. The correction variables used are: $\Delta \ln n_j$ (j = 1 to NG), $\Delta \ln n$, $\Delta \ln T$ and $\pi_i = -\lambda_i/RT$. The large number of equations can be reduced by substituting for $\Delta \ln n_j$. This is achieved by rearranging the Taylor expansion of Equation 4 to give 7:-

$$\Delta \ln n_j = \sum_{i=1}^{l} a_{ij} \pi_i + \frac{H_j^0}{RT} \Delta \ln T + \Delta \ln n - \frac{\mu_j}{RT} \qquad (7)$$

and substituting for $\Delta \ln n_j$ in the Taylor expansions of Equations 4, 5 and 6 to give the required number of linear simultaneous equations of the correction variables.

CONSTRAINING FREE ENERGY

Non equilibrium compositions will have a free energy which is at some value between that of the reactants and the equilibrium products. Therefore to calculate the product composition which has a total free energy of g the following constraint must be placed on the calculation:

$$\sum_{j=1}^{NG} \mu_j n_j - g = 0 \qquad (8)$$

Equation 8 can be thought of as just another condition that must be satisfied at the minimum along with the mass balance Equation 3. Therefore it can be tied to the conditions for a minimum by its own Lagrangian multiplier α, this gives on differentiation with respect to n_j :

$$\sum_{j=1}^{NG} \mu_j + \alpha \sum_{j=1}^{NG} \mu_j + \sum_{j=1}^{NG} \sum_{i=1}^{l} a_{ij} \pi_i = 0 \qquad (9)$$

Equation 9 is the equivalent of Equation 4. The extra variable α will cause an extra column in the matrix therefore an extra equation , the Taylor expansion of Equation 8, is required to

provide the extra row. Taylor expansions and substitutions for $\Delta\ln n_j$ were similar to those for CEA, the iteration variables were $\Delta\ln n$, $\Delta\ln T$, $\Delta\alpha$ and π_i.

Convergence was achieved after an extra relaxation factor was applied to the correction of the natural logarithm of temperature. The validity of the result was confirmed by checking that it gave the correct free energy and that the mass balance was satisfied. The calculated temperature was confirmed by an enthalpy balance calculation. The normal initial estimate for the temperature in CEA is 3800 K, on changing this it was found that the calculated product mixture and temperature changed indicating that the system was insufficiently constrained in that the calculated solution was not unique. It was also noticed that when G was close to that of the reactants the entropy of the products was less than that of the reactants, an impossible result for an irreversible process. It was therefore decided to further constrain the system by fixing its entropy as well as well as its free energy.

CONSTRAINING ENTROPY

The additional constraint was that:

$$\sum_{j=1}^{NG} n_j S_j = s \qquad (10)$$

where s is the set entropy at some value between that of the reactants and that of the equilibrium products. Linking this to the conditions for a minimum via another Lagranian multiplier β gives in as an alternative to Equation 9:

$$\sum_{j=1}^{NG}\mu_j + \alpha\sum_{j=1}^{NG}\mu_j + \beta T\sum_{j=1}^{NG}S_j - \sum_{j=1}^{NG}\sum_{i=1}^{I}a_{ij}\lambda_i = 0 \quad (11)$$

The expression for $\Delta\ln n_j$ obtained from the Taylor expansion of Equation 11 when substituted into the expansions of the other equations gives terms in $\Delta\beta$. The extra equation necessary to obtain a solution was obtained from the Taylor expansion of Equation 10.

Predicting Entropy

The next step was to determine how S varied with G during the course of the reaction. An adiabatic hydrogen/oxygen system with both reactants at 1000 K and 1 bar, and an oxidant to fuel mass ratio of 25.39 was modelled with Sandia's chemical kinetic code CHEMKIN. 1000 K was chosen as the reactant temperature to ensure reaction. The reaction was modelled in a plug flow reactor using the Gas Research Institute H_2/O_2 mechanism. Thermodynamic calculations were carried out on the system composition with time to give plots of both G and S with time as shown in Figures 2 and 3. Figure 4 is a plot of S vs. G.

From the definition of G:-

$$G = H - TS \qquad (12)$$

H is constant (1071.52 KJ/Kg for the above system) and small compared with the changes in G, also the increase in entropy between the reactants and products is small (see Figure 3). Hence G is a linear function of T as is shown in Figure 5; another interpretation is that

$$\left(\frac{\partial G}{\partial T}\right)_P = -S \qquad (13)$$

holds true. Rrearranging Equation 12 gives:

$$S = -\frac{G}{T} + \frac{H^0}{T} \qquad (14)$$

The equilibrium composition and thermodynamic properties of the system can be calculated using CEA, those of the reactants are defined. From these the linear relationship between T and G can be calculated, thus Equation 14 becomes

$$S = \frac{-G + 1071.52}{(-0.07814G + 267.2)} \qquad (15)$$

Figure 6 shows a plot of this function superimposed on Figure 4. Hence, for a set value of G, S can be reasonably predicted.

With the above constraints on G and S the program converged, however, as with the previous version an extra relaxation factor had to be applied to the correction of $\Delta\ln T$. Comparisons of converged solutions with different initial estimates of both temperature and composition still gave differences in the predicted product mole fractions. However these were much reduced being confined to the third significant figure. It appeared that the system had to be further constrained as follows:

Final Constrained Solution

The final constraint applied to tie G and S to the mixture composition was:

$$\sum_{j=1}^{NG}\mu_j n_j = H^0 - T\sum_{j=1}^{NG}S_j n_j \qquad (16)$$

i.e a restatement of Equation 12. This was linked via another multiplier θ to give on differentiation with respect to n_j:

$$\sum_{j=1}^{NS}\mu_j + \alpha\sum_{j=1}^{NS}\mu_j + \beta T\sum_{j=1}^{NS}S_j + \theta\left(T\sum_{j=1}^{NS}S_j + \sum_{j=1}^{NS}\mu_j\right) - \sum_{j=1}^{NS}\sum_{i=1}^{I}a_{ij}n_j\lambda_i \qquad (17)$$

Since G is defined from which S is calculated and H is constant, then from Equation 12, T can be calculated. Therefore T need not be an iteration variable, if it is the system is over-defined. This was probably the cause of convergence instability requiring the extra relaxation factor on the correction of $\Delta\ln T$. The Taylor expansion of Equation 17 for each species

when rearranged in terms of $\Delta \ln n_j$ is:-

$$\Delta \ln n_j = \sum_{i=1}^{l} a_{ij}\pi_i + \Delta \ln n - \frac{\mu_j}{RT}\Delta\alpha - \frac{S_j}{R}\Delta\beta -$$

$$\left(\frac{S_j}{R} + \frac{\mu_j}{RT}\right)\Delta\theta - \frac{\mu_j}{RT} - \frac{\mu_j}{RT}\alpha - \frac{S_j}{R}\beta - \left(\frac{S_j}{R} + \frac{\mu_j}{RT}\right)\theta \qquad (18)$$

Substitution in the Taylor expansions of Equations 3, 5, 6, 8 and 10 gave the iteration equations shown in Appendix 1. The correction variables being: $\Delta \ln n$, $\Delta\alpha$, $\Delta\beta$, $\Delta\theta$ and π_i.

Convergence was achieved without any extra relaxation factors. The standard initial estimate of total number of moles n is 0.1Kg-moles/Kg and n_j = 0.1/NG Kg-moles/Kg. Varying n between 0.05 and 0.2 gave identical solutions to seven significant figures, with convergence limits of 10^{-7} on $\Delta\alpha$, $\Delta\beta$ and $\Delta\theta$. Hence the system was sufficiently constrained to produce a unique solution. Attempts to converge on equilibrium failed, the closest approach was with a free energy set at 0.04% above equilibrium, the results are illustrated in Table 1.

COMPARISON WITH KINETIC CALCULATIONS

The H_2/O_2 system had a reactant and equilibrium free energy of -9648.2 and -33165.7 KJ/Kg of mixture respectively. Non equilibrium compositions with values of G from equilibrium (-33165.7) to -24000 KJ/Kg were calculated and the results compared with those from CHEMKIN in Figures 7 to 15. There is a limit as to how far back the reaction can be tracked, since fixing the value of G and S to that of the reactants does not result in the reactants as products, since they do not represent a local minimum; the program will predict the reactants as products if it is additionally constrained to consider only H_2 and O_2. All the major species, with the exception of OH, show the same concentration trend with G. O_2 and H_2O being particularly close. HO_2, H_2O_2 and O_3 (not shown) have the largest relative divergence, however their absolute concentrations are low. The agreement between temperatures is a reflection of the ability of Equation 15 to predict entropy. Generally non equilibrium mixtures have higher concentrations of free the radicals OH and HO_2 than are found in mixtures calculated with CHEMKIN. The agreement between the two at equilibrium is artificial since CHEMKIN calculations are constrained to converge on equilibrium. Generally with the exception of H_2O_2, HO_2, OH and O_3, non equilibrium concentrations are in reasonable agreement with kinetic predictions as is also the temperature. Interestingly attempts to obtain convergence at the G and S of CHEMKIN mixtures failed. The CHEMKIN conditions were found to be outside the solution domain of the non equilibrium program; this was probably due to the entropy of the CHEMKIN products being high, see Figure 6, e.g. CHEMKIN equilibrium entropy was 11.9901 compared to CEA's 11.9762 KJ/Kg-K. Also the enthalpy of the CHEMKIN mixture which was slightly higher than that of the reactants thus Equation 6 could not be satisfied.

DERIVATION OF THE EXTENT OF REACTION

The above non equilibrium predictions do tell us in terms of free energy how far from equilibrium the system is, but give us no information about the (thermodynamic) reaction progress variable extent of reaction.

Extent of Reaction and Affinity

Consider the general chemical reaction

$$\nu_1 B_1 + \nu_2 B_2 + \ldots\ldots \rightarrow \nu_n B_n + \nu_{n+1} B_{n+1} + \ldots\ldots \qquad (19)$$

it can be briefly written as

$$\sum \nu_j B_j = 0 \qquad (20)$$

since by convention the stoichiometric mole numbers n_j are positive for products and negative for reactants. If we denote the reaction progress variable by the symbol ξ. A change from ξ to $\xi + d\xi$ means that $\nu_1\, d\xi$ moles of B_1, $\nu_2\, d\xi$ of B_2, etc. have reacted to form $\nu_n\, d\xi$ moles of B_n, etc. Thus ξ is a convenient measure of the extent of reaction. The number of moles reacted of any component j is

$$dn_j = \nu_j d\xi \qquad (21)$$

Since

$$\delta G = \sum \mu_j \delta n_j \qquad (22)$$

then

$$\frac{dG}{d\xi} = \sum \nu_j \mu_j \qquad (23)$$

The term $-\sum \nu_j \mu_j$ is a function of state called affinity (A) (De Donder 1920), at equilibrium A=0. -A is also the slope of the function $G = f(\xi)$. It can also be shown that for an irreversible process

$$\frac{\partial^2 G}{\partial \xi^2} \geq 0 \qquad (24)$$

(Prigogine 1952), therefore $f(\xi)$ is concave. Hence the plot of G against ξ will be hyperbolic in nature the curve being asymptotic to the equilibrium value of G (Ge). From the non equilibrium program the product composition and temperature at any point along the curve can be calculated so therefore can the slope $\sum \nu_j \mu_j$. Equation 23 in discrete form is:

$$\frac{\Delta G}{\Delta \xi} = \sum \nu_j \mu_j \qquad (25)$$

hence if ΔG and $\sum \nu_j \mu_j$ are known then $\Delta\xi$ can be calculated. Since the function relating G and ξ is hyperbolic and asymptotic to the equilibrium free energy (Ge) then it may be of the form:

$$G = \frac{C}{\xi} + G_e \qquad (26)$$

where C is a constant. Re-arranging Equation 26 gives:

$$\Delta\xi = \xi_1 - \xi_2 = C\left(\frac{1}{G_1 - G_e} - \frac{1}{G_2 - G_e}\right) \qquad (27)$$

Therefore a plot of $1/(G_1 - G_e) - 1/(G_2 - G_e)$ vs. $\Delta\xi$ should be a straight line of slope C. Linear plots were obtained for several values of ΔG, Figures 16 and 17 show how the slope and intercept varied with the step value of G. As ΔG decreases so the slope approaches a constant value and the intercept approaches zero. Figure 18 shows the plot of Equation 27 for the smallest ΔG, 5 KJ/Kg. Hence Equation 26 becomes:

$$G = \frac{4699}{\xi} + G_e \qquad (28)$$

Equation 28 will converge at Ge when ξ is infinite. When ξ is zero G is infinite and not the free energy of the reactants (Gr). To overcome this the curve has to be offset by the value of zeta when G = Gr denoted ξr. Therefore the final forms of the equations are:

$$G = \frac{4699}{\xi + \xi_r} + G_e \qquad (29)$$

and

$$\xi = \frac{4699}{G - G_e} - \xi_r \qquad (30)$$

Composition Changes with Extent of Reaction

Figure 19 shows the plot of Equation 29 for the hydrogen/oxygen system under consideration. Being now able to calculate the function relating the extent of reaction and the systems free energy, from the free energy and non equilibrium composition, species concentration plots against ξ can be derived. Figures 20 and 21 show some typical concentration plots and Figure 22 the temperature plot. The plot of mole fraction of water vs. zeta is also hyperbolic in nature and could be represented by an equation of the type:

$$[H_2O] = -\frac{B}{\xi} + [H_2O]_e \qquad (31)$$

where $[H_2O]_e$ is the mole fraction of water at equilibrium and B is a constant. For products that decrease with ξ the minus in Equation 31 would be replaced by a plus.

APPLICATION TO CHEMICAL MODELS

The above non equilibrium solution for the H_2/O_2 system could be used to model premixed, undiluted, combustion. However the majority of practical combustion devices are not premixed, being based on laminar or turbulent diffusion flames. In order to model the chemistry in such flames an extra dimension, mf or o/f, has to be included. Figures 23 to 25 illustrate such a three dimensional model. o/f ratios were varied from 5 to 40, Equation 29 was derived for a series of o/F's and the two dimensional ξ product concentration plots were constructed and amalgamated into three dimensional plots. Since ξ varied over a wide range it was plotted in logarithmic form. Reactant surface plots, such as H_2, are concave whilst product surfaces, H_O, are convex. Intermediate surfaces, OH, have both concave and convex regions. The planes marked 'A' represent the conventional two dimensional equilibrium model.

All non equilibrium models e.g. those based on chemical kinetics or laminar flamelets require experimental data for their construction. A non equilibrium thermodynamic model is no exception, since in order to predict the product mixture properties a value of ξ has to be assigned to each calculation node in the flow field. Therefore it is of interest to investigate what correlates with ξ to aid its prediction.

Since G is a function of time (see Figure 3) and ξ is a function of G, then ξ must be a function of time (t). The ξ values corresponding to the G values from the kinetic simulation were plotted against t. The kinetic simulation relied on autoignition, whereas in a continuous combustion system incoming fuel and oxidant are ignited by recirculated combustion products. To simulate this the ignition delay time was subtracted from t. The resulting plot is shown in Figure 26 together with the best fit obtained. Figure 27 illustrates how the exponential form holds over the whole data range. If the relationship is exponential then since when ξ = 0 t = 0 theoretically it should be of the form:

$$\xi = e^{bt} - 1 \qquad (32)$$

where 'b' is a constant for a given o/f ratio and reactant temperature and pressure, this is close to the fit in Figure 26. Therefore with experimental values of 'b', ξ could be determined from residence time.

Residence time and its pdf are not solution variables in current CFD codes, they can only be inferred by post processing techniques such as particle tracking. A more empirical approach would be to correlate ξ with mf. Measurements such as those shown in Figure 1 indicate that ξ is furthest from equilibrium in rich regions and closest in lean regions. Actual flame species measurements could therefore be used to evaluate how ξ varies with mf.

CONCLUSIONS

A method of obtaining non equilibrium thermodynamic product compositions and properties, by constraining free energy and entropy, has been developed for constant pressure combustion.

Compositions calculated thermodynamically and those calculated from kinetic data are in reasonable agreement.

It is demonstrated that from the calculated compositions it is possible to derive the thermodynamic progress variable, extent of reaction, and how it varies with the systems free energy. Thus how compositions and temperature vary with extent of reaction can also be determined. These two dimensional plots can be expanded to three dimensional surfaces applicable to lamina or turbulent diffusion flames.

For a given combustion system extents of reaction may be derived from local residence times or mixture fractions.

Acknowledgements

This work was carried out as part of Technology Group 3 of the UK Ministry of Defence Corporate Research Programme. The authors would also like to acknowledge Bonnie J. McBride, NASA Lewis Research Centre, for providing the source code and program documentation and R. E. Seoud DERA for his advice during this project.

References

DE Donder T., Lecons de Thermodynamique et de Chimie-Physique, Gauthier-Villars, Paris, 1920.

Gordon S. and McBride B. J., Computer Program for Calculation of Complex Chemical Equilibrium Compositions and Applications, NASA Reference Publication 1311, Oct., 1994.

Prigogine I. and Defray R., Translated by Everett D. H., Chemical Thermodynamics, Longmans, p81, 1952.

Hurley C. D., Internal Mapping of a Single Annular Airspray Combustor, Report No, DRA/AS/PTD/CR/94265/1, 1994.

	Equilibrium	Nearest Converged Solution
Calculated Temperature K	2858.78	2857.56
Calculated G KJ/Kg	-33165.7	-33151.0
Calculated S KJ/Kg-K	11.9762	11.9761
Mole Fractions H	0.01229	0.01223
HO2	0.00011	0.00021
H2	0.01518	0.01606
H2O	0.37994	0.37895
H2O2	0.0	0.0
O	.04567	.04494
OH	0.09072	0.09086
O2	0.45608	0.45672
O3	0.0	0.0

Table 1. Comparison of Equilibrium with the Nearest Non Equilibrium Converged Solution.

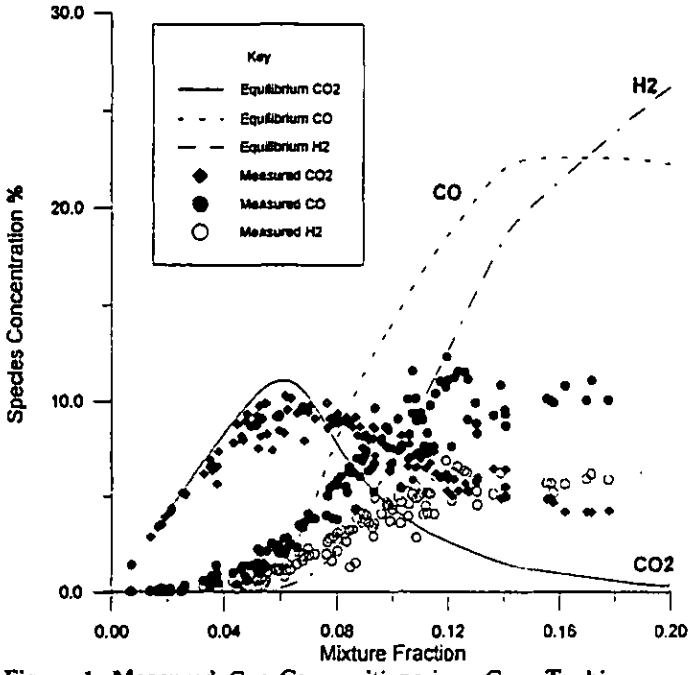

Figure 1. Measured Gas Compositions in a Gas Turbine Primary Zone Compared to Equilibrium.

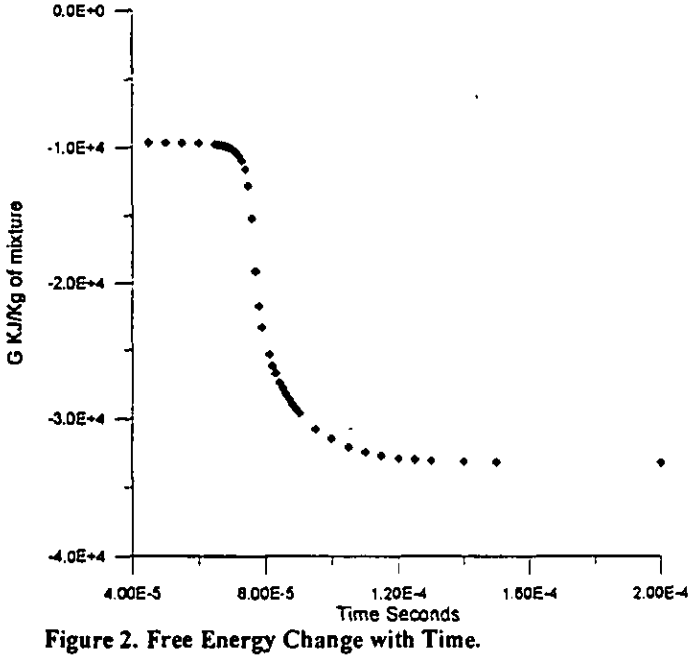

Figure 2. Free Energy Change with Time.

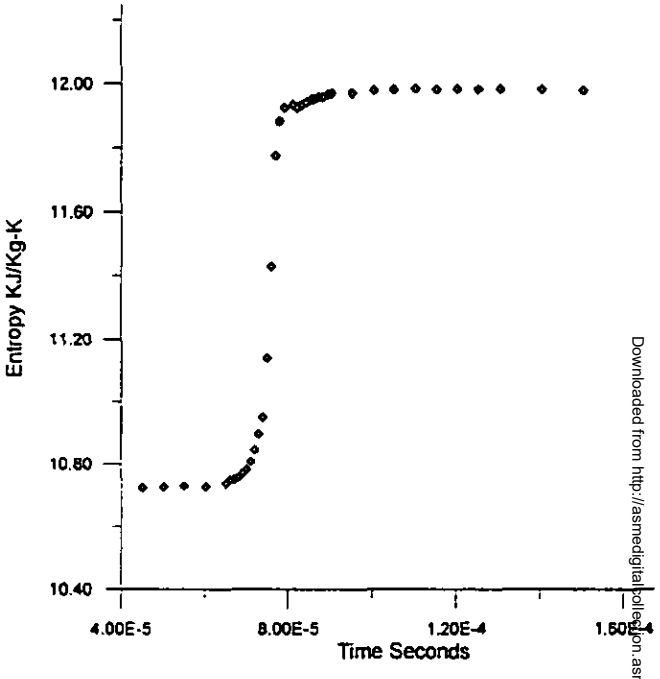

Figure 3. Entropy Change with Time.

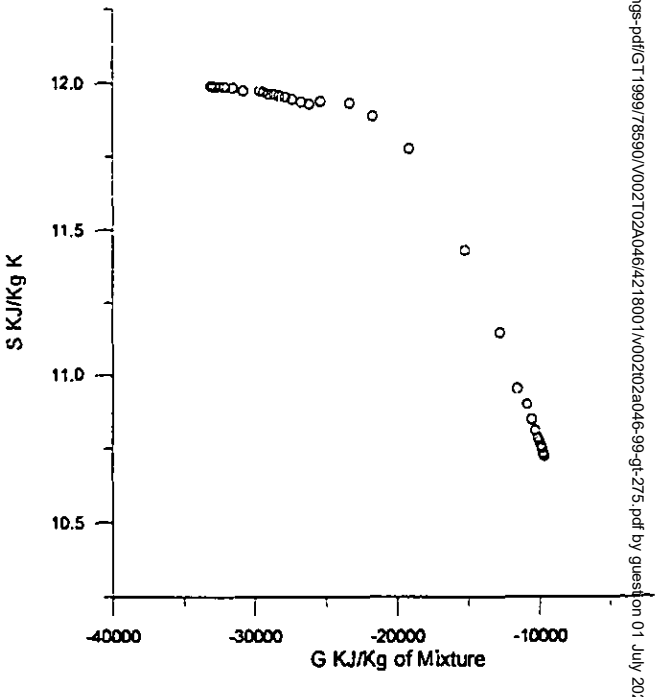

Figure 4. Free Energy vs Entropy.

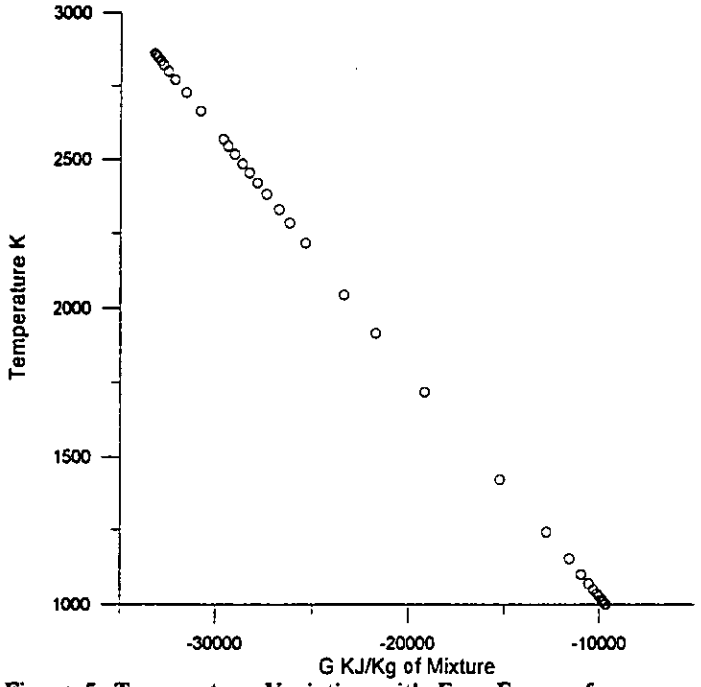

Figure 5. Temperature Variation with Free Energy from Chemkin Simulation.

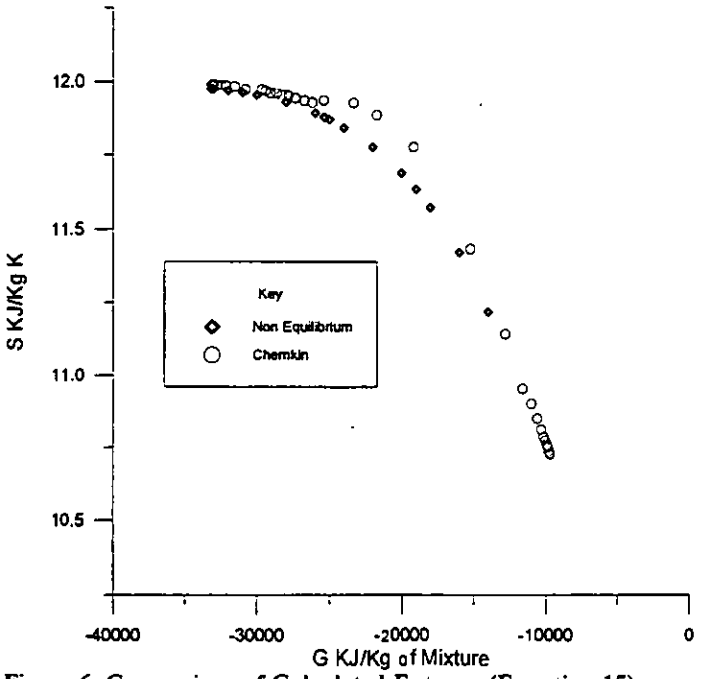

Figure 6. Comparison of Calculated Entropy (Equation 15) with CHEMKIN Predictions.

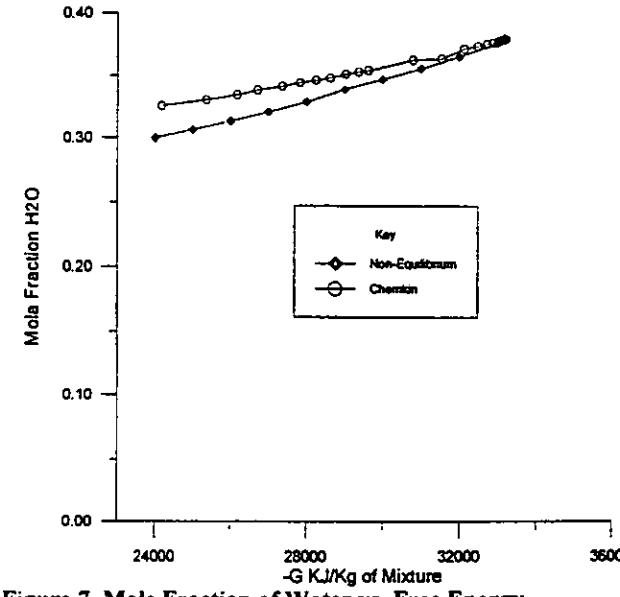

Figure 7. Mole Fraction of Water vs. Free Energy.

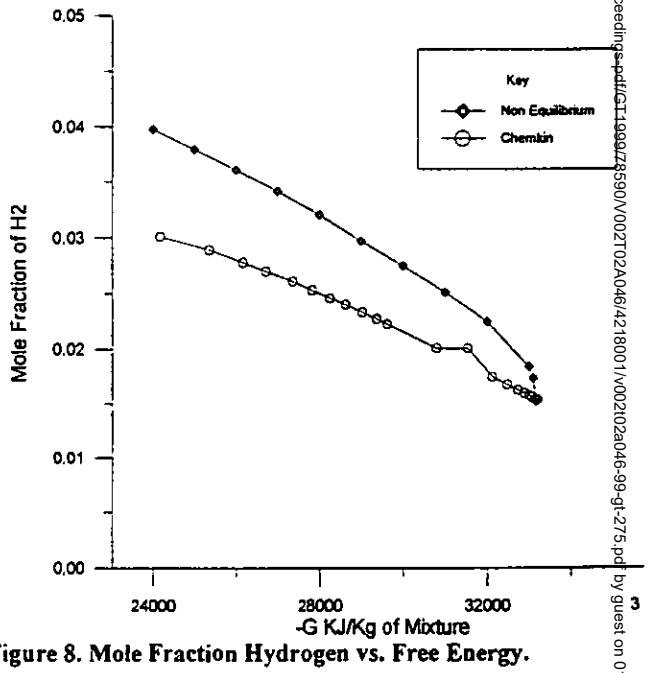

Figure 8. Mole Fraction Hydrogen vs. Free Energy.

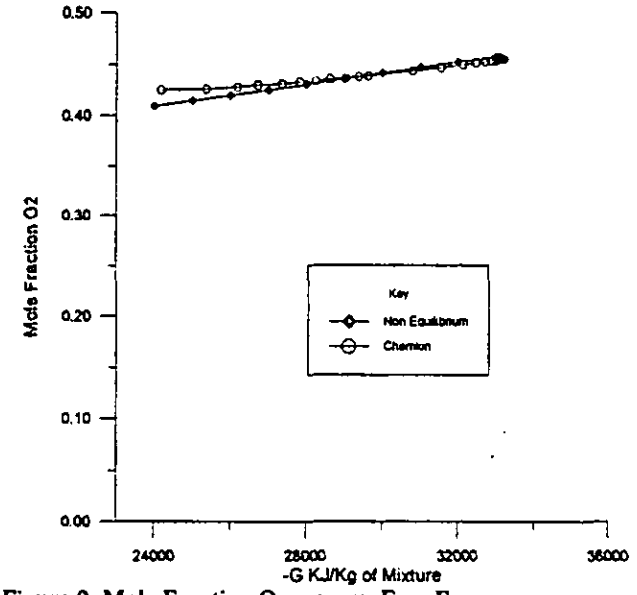

Figure 9. Mole Fraction Oxygen vs. Free Energy.

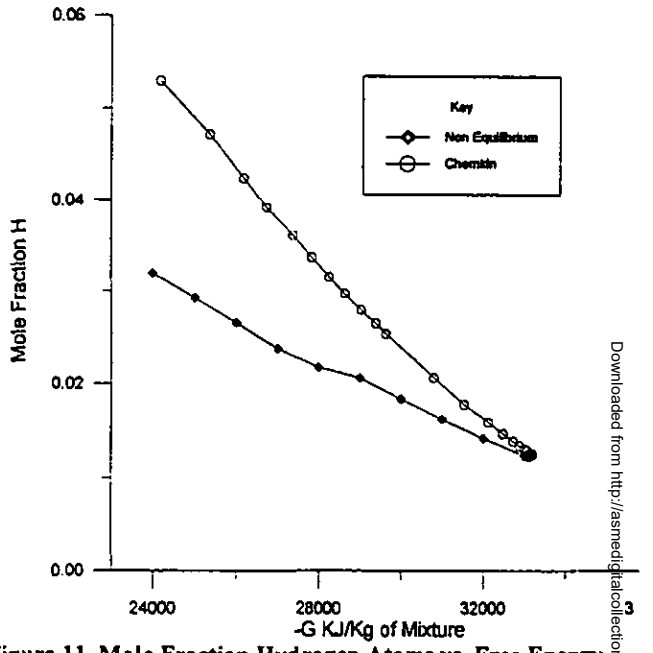

Figure 11. Mole Fraction Hydrogen Atoms vs. Free Energy.

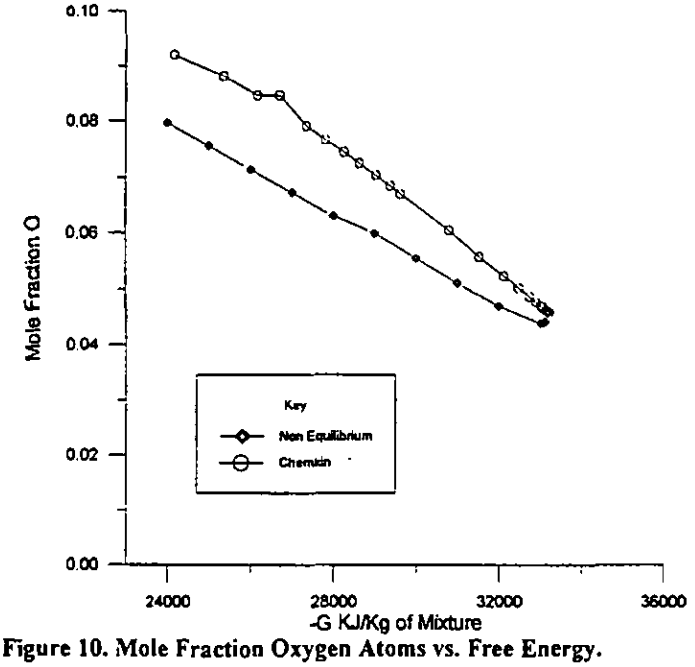

Figure 10. Mole Fraction Oxygen Atoms vs. Free Energy.

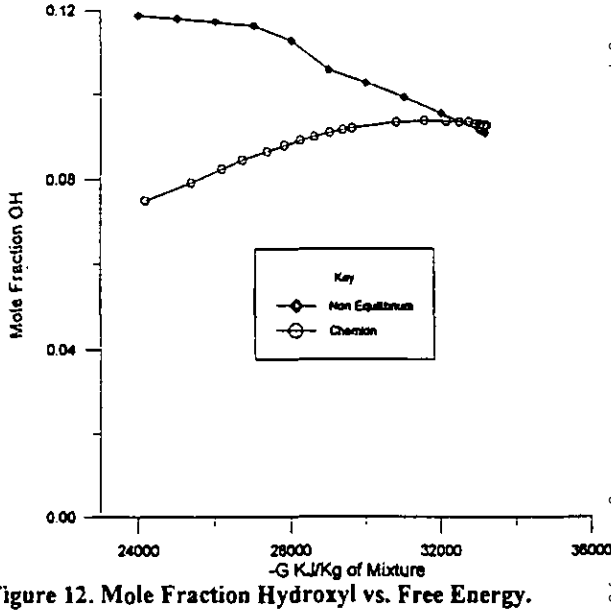

Figure 12. Mole Fraction Hydroxyl vs. Free Energy.

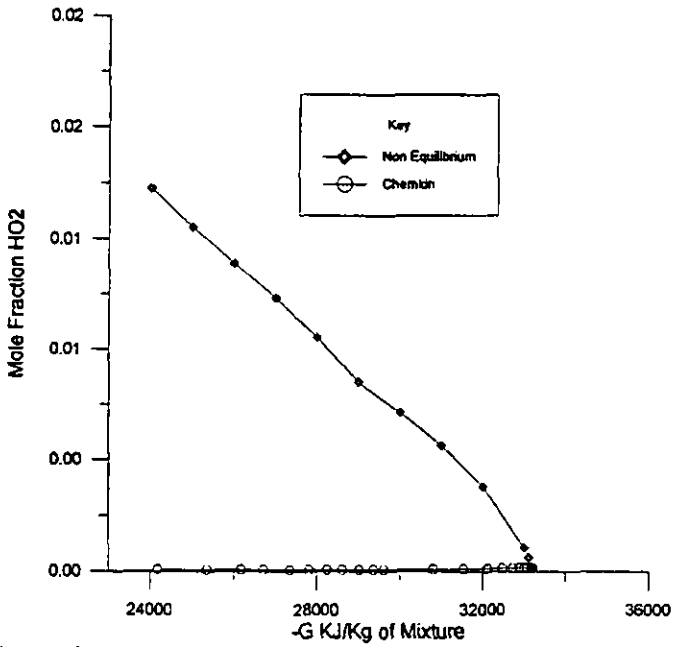

Figure 13. Mole Fraction Hydroperoxy vs Free Energy.

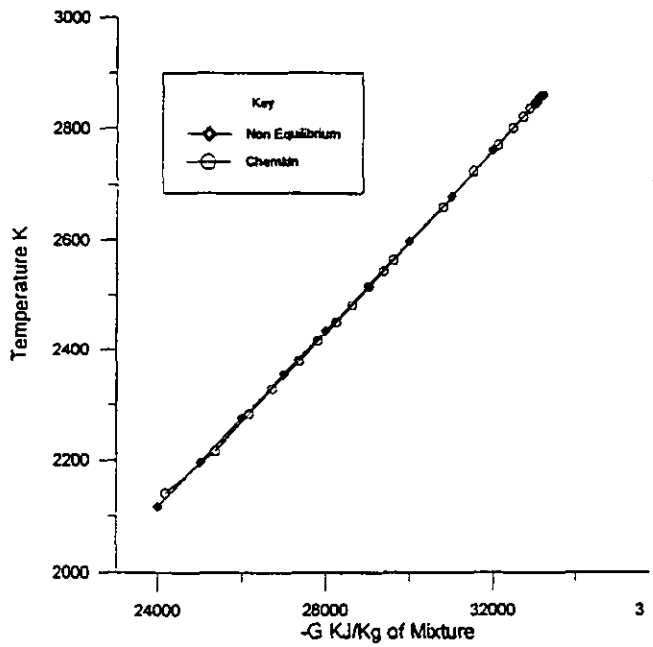

Figure 15. Temperature K vs. Free Energy.

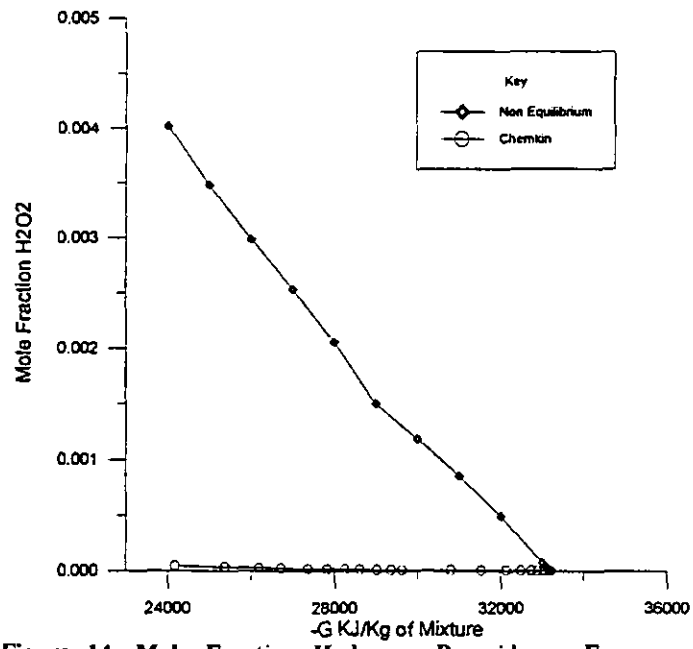

Figure 14. Mole Fraction Hydrogen Peroxide vs Free Energy.

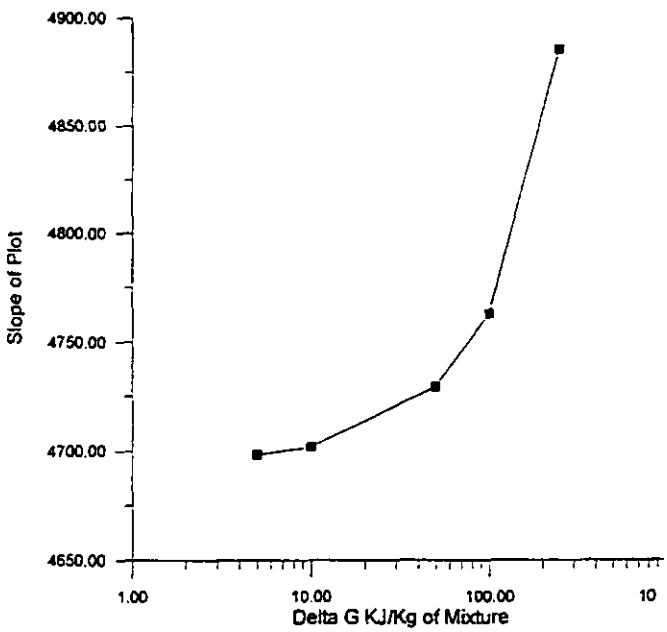

Figure 16. Slope vs. Step Size of ΔG.

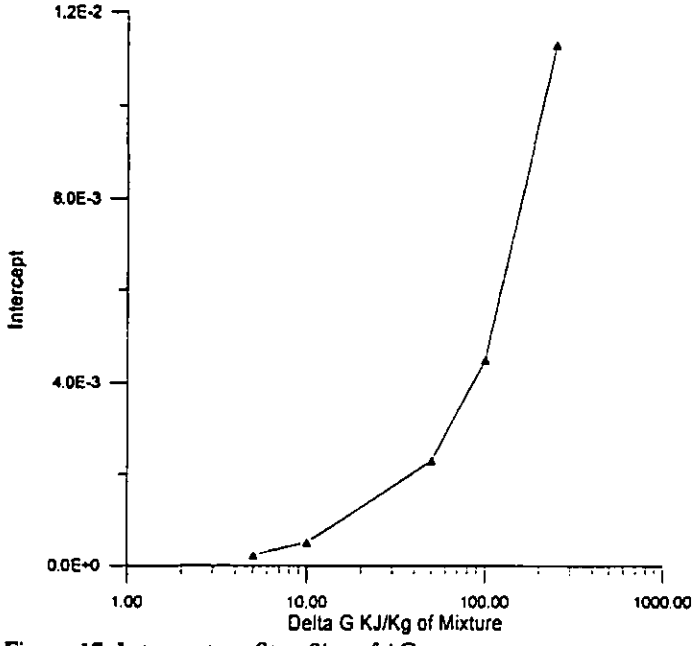

Figure 17. Intercept vs. Step Size of ΔG.

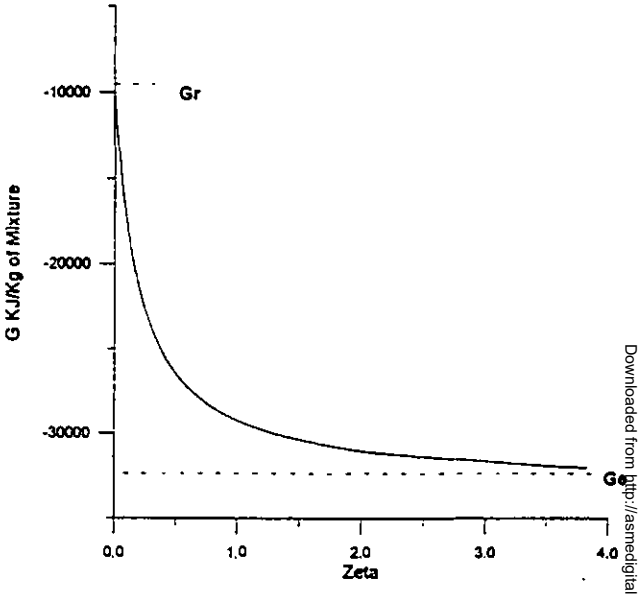

Figure 19. Free Energy vs. Extent of Reaction.

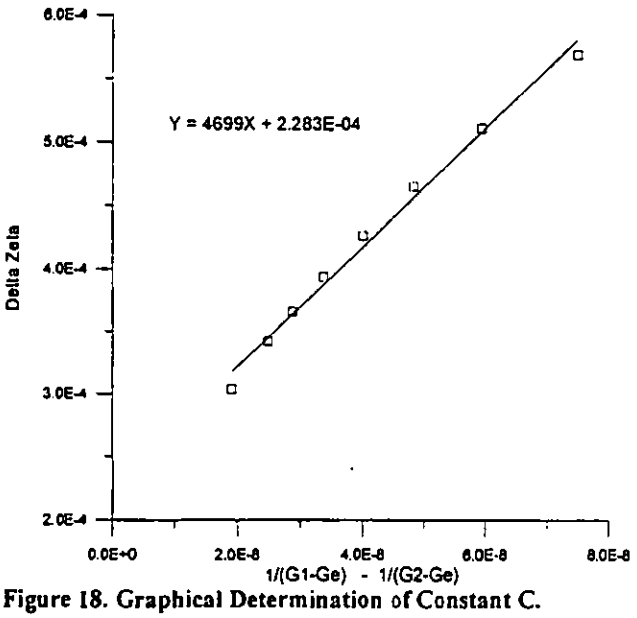

Figure 18. Graphical Determination of Constant C.

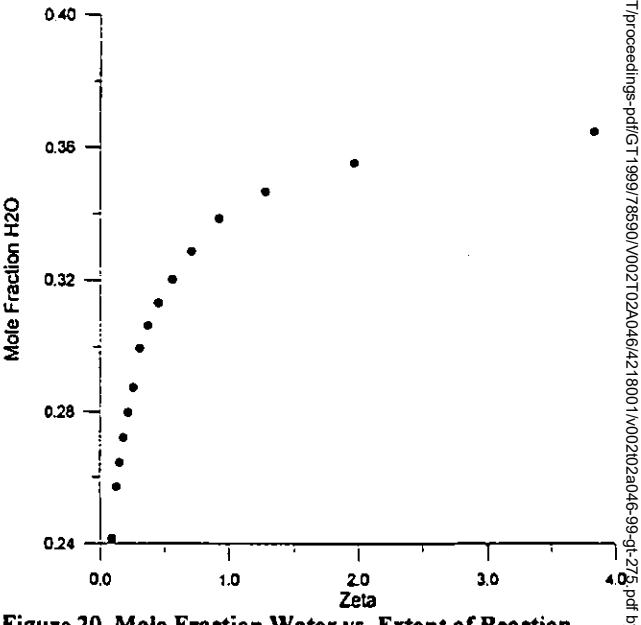

Figure 20. Mole Fraction Water vs. Extent of Reaction.

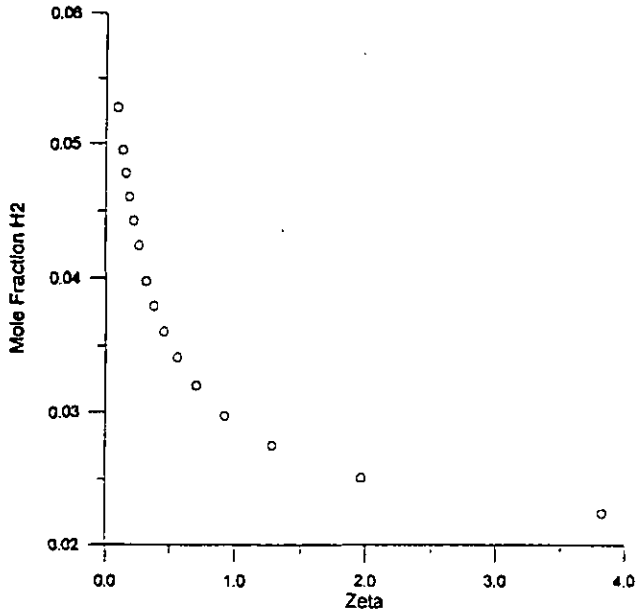

Figure 21. Mole Fraction Hydrogen vs. Extent of Reaction.

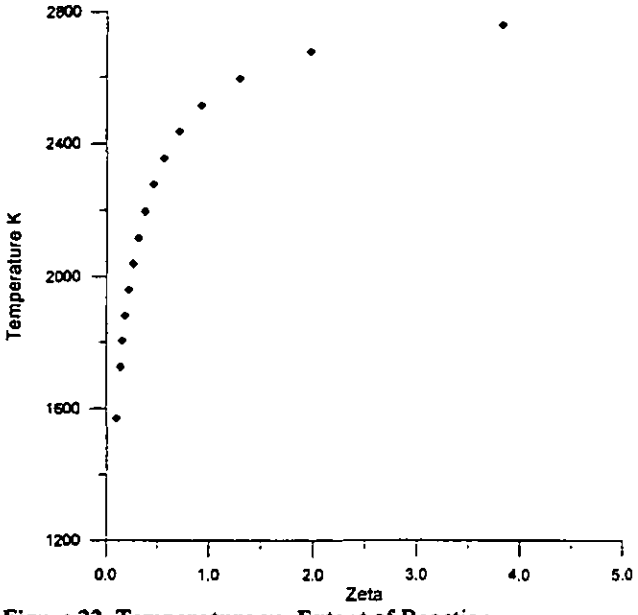

Figure 22. Temperature vs. Extent of Reaction.

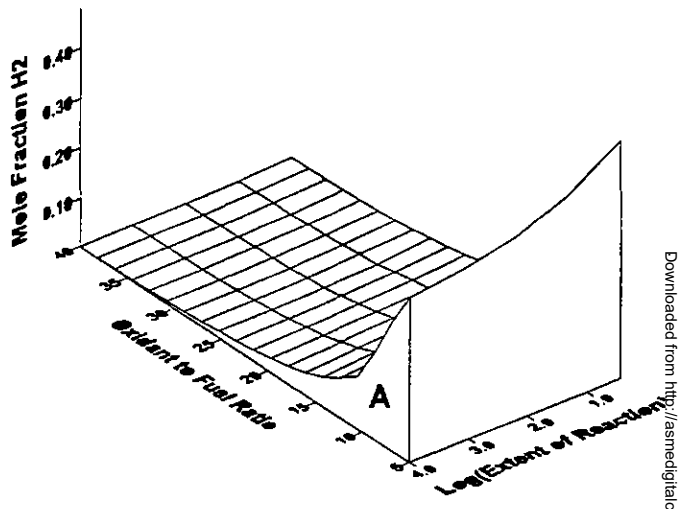

Figure 23. Reactant Surface.

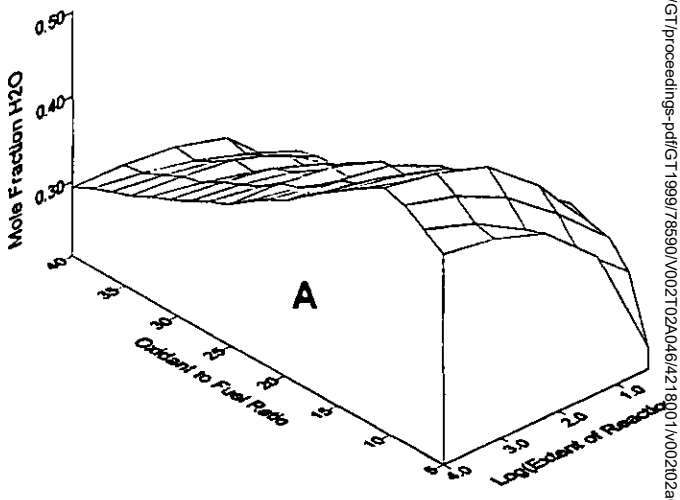

Figure 24. Product Surface.

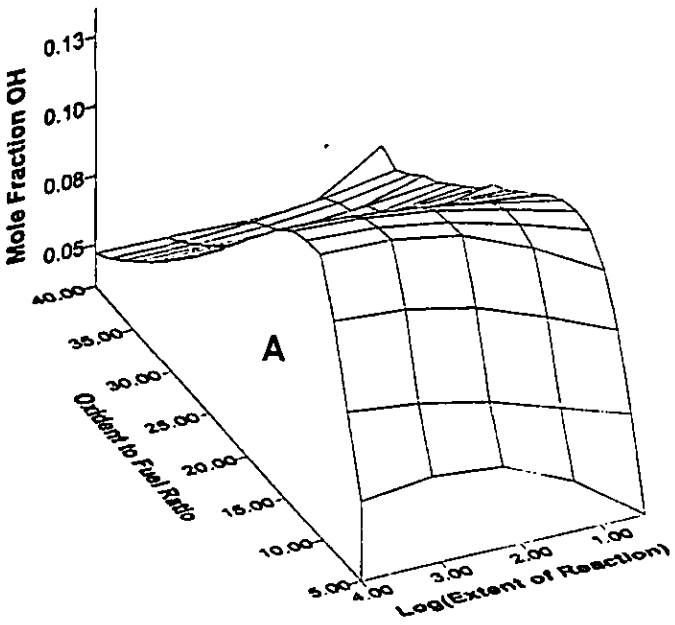

Figure 25. Intermediate Surface.

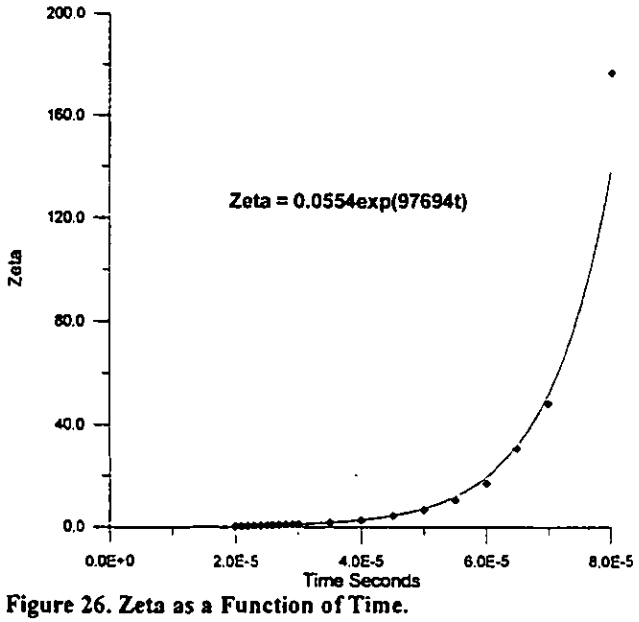

Figure 26. Zeta as a Function of Time.

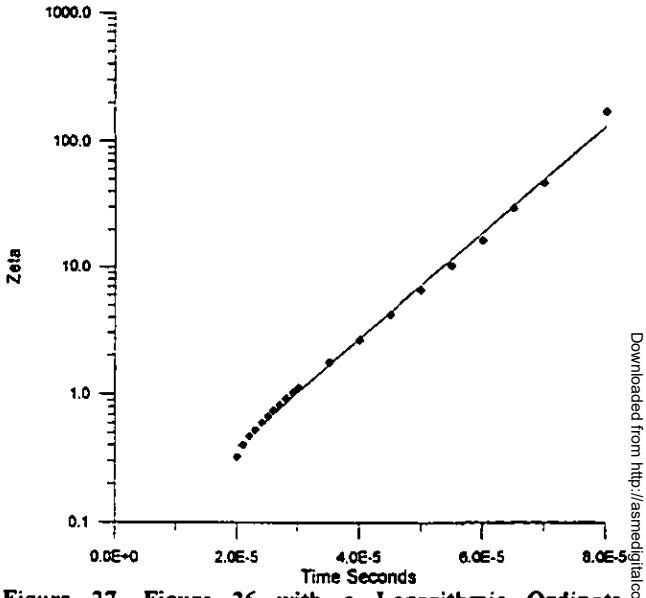

Figure 27. Figure 26 with a Logarithmic Ordinate.

APPENDIX 1

Iteration Equations from Taylor Expansions

Equation 3

$$\sum_{j=1}^{NG}\sum_{i=1}^{I} a_{ij}a_{kj}n_j\pi_i + \sum_{j=1}^{NG} a_{ij}n_j\Delta\ln n - \sum_{j=1}^{NG} a_{ij}\frac{\mu_j}{RT}n_j\Delta\alpha - \sum_{j=1}^{NG} a_{ij}\frac{S_j}{R}n_j\Delta\beta$$

$$-\sum_{j=1}^{NG} a_{ij}\left(\frac{S_j}{R}+\frac{\mu_j}{RT}\right)n_j\Delta\theta = b_i^0 - b_i + \sum_{j=1}^{NG} a_{ij}\left(\frac{\mu_j}{RT}(1+\alpha)+\frac{S_j}{R}\beta+\left(\frac{S_j}{R}+\frac{\mu_j}{RT}\right)\theta\right)n_j$$

Equation 5

$$\sum_{j=1}^{NG}\sum_{i=1}^{I} a_{ij}n_j\pi_i + \left(\sum_{j=1}^{NG} n_j - n\right)\Delta\ln n - \sum_{j=1}^{NG}\frac{\mu_j}{RT}n_j\Delta\alpha - \sum_{j=1}^{NG}\frac{S_j}{R}n_j\Delta\beta - \sum_{j=1}^{NG}\left(\frac{S_j}{R}+\frac{\mu_j}{RT}\right)n_j\Delta\theta =$$

$$n - \sum_{j=1}^{NG} n_j + \sum_{j=1}^{NG}\left(\frac{\mu_j}{RT}(1+\alpha)+\frac{S_j}{R}\beta+\left(\frac{S_j}{R}+\frac{\mu_j}{RT}\right)\theta\right)n_j$$

Equation 6

$$\sum_{j=1}^{NG}\sum_{i=1}^{I} a_{ij}\frac{H_j^0}{RT}n_j\pi_i + \sum_{j=1}^{NG}\frac{H_j^0}{RT}n_j\Delta\ln n - \sum_{j=1}^{NG}\frac{H_j^0\mu_j}{RTRT}n_j\Delta\alpha - \sum_{j=1}^{NG}\frac{H_j^0 S_j}{RTR}n_j\Delta\beta - \sum_{j=1}^{NG}\frac{H_j^0}{RT}\left(\frac{S_j}{R}+\frac{\mu_j}{RT}\right)n_j\Delta\theta =$$

$$\frac{H}{RT} - \frac{H^0}{RT} + \sum_{j=1}^{NG}\frac{H_j^0}{RT}\left(\frac{\mu_j}{RT}(1+\alpha)+\frac{S_j}{R}\beta+\left(\frac{S_j}{R}+\frac{\mu_j}{RT}\right)\theta\right)n_j$$

Equation 8

$$\sum_{j=1}^{NG}\sum_{i=1}^{I} a_{ij}\left(\frac{\mu_j}{RT}+1\right)n_j\pi_i + \sum_{j=1}^{NG}\frac{\mu_j}{RT}n_j\Delta\ln n - \sum_{j=1}^{NG}\frac{\mu_j}{RT}\left(\frac{\mu_j}{RT}+1\right)n_j\Delta\alpha - \sum_{j=1}^{NG}\frac{S_j}{R}\left(\frac{\mu_j}{RT}+1\right)n_j\Delta\beta$$

$$-\sum_{j=1}^{NG}\left(\frac{S_j}{R}+\frac{\mu_j}{RT}\right)\left(\frac{\mu_j}{RT}+1\right)n_j\Delta\theta = \frac{g}{RT} - \sum_{j=1}^{NG}\frac{\mu_j}{RT}n_j + \sum_{j=1}^{NG}\left(\frac{\mu_j}{RT}+1\right)\left(\frac{\mu_j}{RT}(1+\alpha)+\frac{S_j}{R}\beta+\left(\frac{S_j}{R}+\frac{\mu_j}{RT}\right)\theta\right)n_j$$

Equation 10

$$\sum_{j=1}^{NG}\sum_{i=1}^{I} a_{ij}\frac{S_j}{R}n_j\pi_i + \sum_{j=1}^{NG}\frac{S_j}{R}n_j\Delta\ln n - \sum_{j=1}^{NG}\frac{S_j\mu_j}{RRT}n_j\Delta\alpha - \sum_{j=1}^{NG}\frac{S_jS_j}{RR}n_j\Delta\beta - \sum_{j=1}^{NG}\frac{S_j}{R}\left(\frac{S_j}{R}+\frac{\mu_j}{RT}\right)n_j\Delta\theta =$$

$$\frac{s}{R} - \sum_{j=1}^{NG}\frac{S_j}{R}n_j + \sum_{j=1}^{NG}\frac{S_j}{R}\left(\frac{\mu_j}{RT}(1+\alpha) + \frac{S_j}{R}\beta + \left(\frac{S_j}{R}+\frac{\mu_j}{RT}\right)\theta\right)n_j + n - \sum_{j=1}^{NG}n_j$$